X. PHYSICAL ACOUSTICS*

Academic Research Staff

Prof. K. U. Ingard

Graduate Students

C. M. Christensen
A. G. Galaitsis
J. A. Tarvin

RESEARCH OBJECTIVES

Our general objective involves the study of the emission, propagation, and absorption of acoustic waves in matter. Specific areas of present research include (i) the interaction of waves with coherent light beams in fluids and solids, (ii) nonlinear acoustics in fluids, and (iii) the generation and propagation of sound waves in moving fluids, with particular emphasis on waves propagated in ducts and generation of sound by turbulent flow.

K. U. Ingard

A. ON THE PROPAGATION OF SOUND IN A DUCT WITH FLOW

In order to illustrate some basic features of sound transmission in a duct with steady flow, we shall consider first the simple case of transmission between two plane-parallel plates so that only two space coordinates (x and y) will be involved in the description of the field. The circumstances are illustrated in Fig. X-1. The flow is assumed to

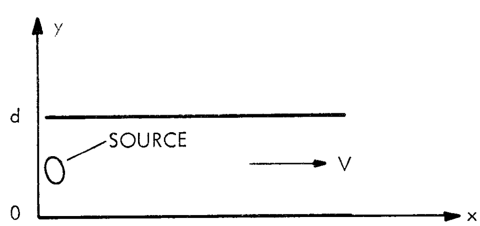

Fig. X-1. Duct with boundaries at $y = 0$ and $y = d$ carrying uniform flow of velocity V. The sound source is stationary and periodic with frequency $\omega/2\pi$.

be uniform, with velocity V in the x direction. The width of the duct is d, and the boundaries are rigid. The source is stationary with respect to the duct. We shall consider a simple harmonic source of frequency $\omega/2\pi$.

1. Doppler Shift

In a coordinate system (y, x_1) moving with the flow the medium is stationary, and the wave field is determined from the standard wave equation $\partial^2 p/\partial t^2 = c^2\nabla_1^2 p$, where

*This work was supported principally by the U.S. Navy (Office of Naval Research) under Contract N00014-67-A-0204-0019; and in part by the Joint Services Electronics Program (Contract DAAB07-71-C-0300).

∇_1 refers to the (y, x_1) system. For harmonic time dependence $\exp(-i\omega t)$ we have $\partial^2 p/\partial t^2 = -\omega_1^2 p$. The wave field of interest in this problem must then be of the form

$$p = A \cos (k_y d) \exp(ik_x x_1 - i\omega_1 t), \tag{1}$$

where $x_1 = x - Vt$, and $\omega_1/2\pi$ is the frequency as measured in this coordinate system. Since in this system the observer is moving relative to the source, the frequency is Doppler-shifted. It follows from the wave equation that the propagation constant k_x is given by

$$k_x^2 = (\omega_1/c)^2 - k_y^2. \tag{2}$$

For rigid boundaries we have $k_y = n\pi/d$, where n is an integer designating the mode number.

If we introduce $x_1 = x - Vt$ into Eq. 1, the argument of the exponential function becomes $(ikx - \omega t)$, where

$$\omega = \omega_1 + k_x V. \tag{3}$$

In other words, the Doppler shift depends on k_x, and consequently is different for different modes.

2. Dispersion Relation

Since, according to Eq. 2, k_x depends on ω_1, we can express the relation between k_x and ω by inserting $\omega_1 = \omega - k_x V$ into Eq. 2. Solving for k_x then yields

$$(1-M^2)k_x/(\omega/c) = -M \pm \sqrt{1 - k_y^2(1-M^2)/(\omega/c)^2}. \tag{4}$$

This may be regarded as the dispersion relation $\omega = \omega(k_x)$ for the wave modes propagating in the x direction. This relation can be obtained also from the wave equation

$$\left(\frac{\partial}{\partial t} + V \frac{\partial}{\partial x}\right)^2 p = c^2 \nabla^2 p,$$

which is obtained from the ordinary wave equation $\partial^2 p/\partial t^2 = c^2 \nabla_1^2 p$ by the coordinate transformation $x_1 = x - Vt$.

3. Phase and Group Velocity

The phase velocity is obtained from Eq. 4:

$$v_p = \omega/k_x, \tag{5}$$

and for the group velocity we obtain

$$v_{gx} = \frac{d\omega}{dk_x} = \frac{c(1-M^2)\sqrt{1-(1-M^2)(k_y c/\omega)^2}}{\pm 1 - M\sqrt{1-(1-M^2)(k_y c/\omega)^2}}. \tag{6}$$

4. Geometrical Interpretation

The expressions for the phase and group velocities, from Eqs. 4-6, are consistent with the simple geometrical interpretation that follows directly from realizing that the wave field in the duct can be regarded as the superposition of plane waves. The direction of propagation of these waves depends on which mode is being considered. The mode is determined by the value of k_y, which in the case of rigid duct walls, as we have seen, is $k_y = n\pi/d$, corresponding to zero normal velocity at the boundary. Thus if we introduce the angle defined by

$$\tan\phi = k_y/k_x, \tag{7}$$

the mode defined by k_y and k_x can be regarded as the superposition of two plane waves traveling in directions that make angles $+\phi$ and $-\phi$ with the x axis, as shown in Fig. X-2. For a plane wave traveling in the $+\phi$ direction in a fluid that moves with a velocity V in the x direction the surfaces of constant phase move in the ϕ direction with a velocity

$$v = c + V\cos\phi. \tag{8}$$

This is the sum of the local speed of sound and the projection of the fluid velocity upon the direction of propagation, as indicated in Fig. X-2. The intersection of the phase front with the x axis (and hence with the duct wall) moves in the x direction with velocity

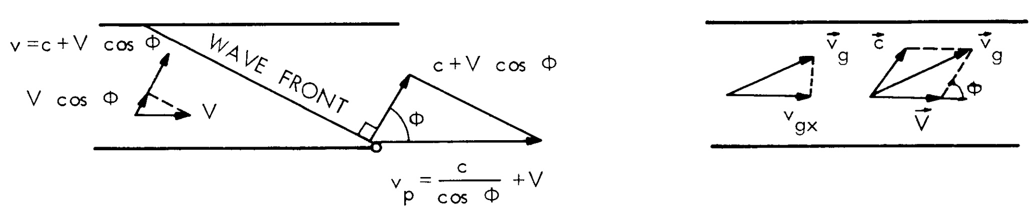

Fig. X-2. Higher modes in the duct can be regarded as a superposition of plane waves traveling in directions that make angles $+\phi$ and $-\phi$ with the x axis, where $\tan\phi = k_y/k_x$. The phase velocity of each elementary wave is $c+V\cos\phi$, and the corresponding trace velocity along the x axis $V+c/\cos\phi$ is the phase velocity of the corresponding duct mode. The group velocity of the individual waves is $v_g = c+V$, and its component along the x axis $v_{gx} = c\cos\phi+V$ is the group velocity of the duct mode.

$$v_p = \frac{c}{\cos\phi} + V. \tag{9}$$

If we introduce the expression for ϕ given in Eq. 7, we find that this velocity is identical with the phase velocity given by Eqs. 4 and 5. Also, as expected, the group velocity v_{gx} given in Eq. 6 equals the x component of $\vec{v}_g$, the vector sum of $\vec{c}$ and $\vec{V}$, where $\vec{c}$ is the velocity-of-sound vector pointing in the direction of propagation. Thus

$$v_{gx} = c \cos\phi + V. \tag{10}$$

5. Discussion of Cutoff Conditions with Group and Phase Velocities

Cutoff condition. In the expression for k_x in Eq. 4 the plus and minus signs signify two possible solutions which in the absence of flow merely refer to the waves propagating in the positive and negative x directions, that is, with positive and negative values of the phase and group velocities. In the presence of flow this interpretation is valid only with regard to the group velocity. As it turns out, the phase velocity can be negative, even if the group velocity is positive. To understand this behavior, we make use of the geometrical interpretation in the discussion of the dispersion relation in Eq. 4.

For the plane wave, k_y equals zero and the propagation constant k_x is real for all values of ω. For higher order modes (k_y different from zero) propagation occurs only if $\omega > \omega_c$, where

$$\omega_c/c = k_y\sqrt{1-M^2}. \tag{11}$$

The corresponding value of k_x is

$$k_x = -(\omega_c/c)M/(1-M^2) = -k_yM\Big/\sqrt{1-M^2}$$

and

$$\tan\phi = -\frac{\sqrt{1-M^2}}{M} = -\frac{\sqrt{c^2-M^2}}{V}. \tag{12}$$

The geometrical interpretation of this result is shown in Fig. X-3. We see that at cutoff the phase velocity is negative, but the angle of propagation of the elementary plane wave is such as to make the group velocity zero (the total group velocity vector $\vec{v}_g$ is perpendicular to the duct). The zero value of the group velocity at cutoff is seen to be consistent also with the analytical expression in Eq. 6.

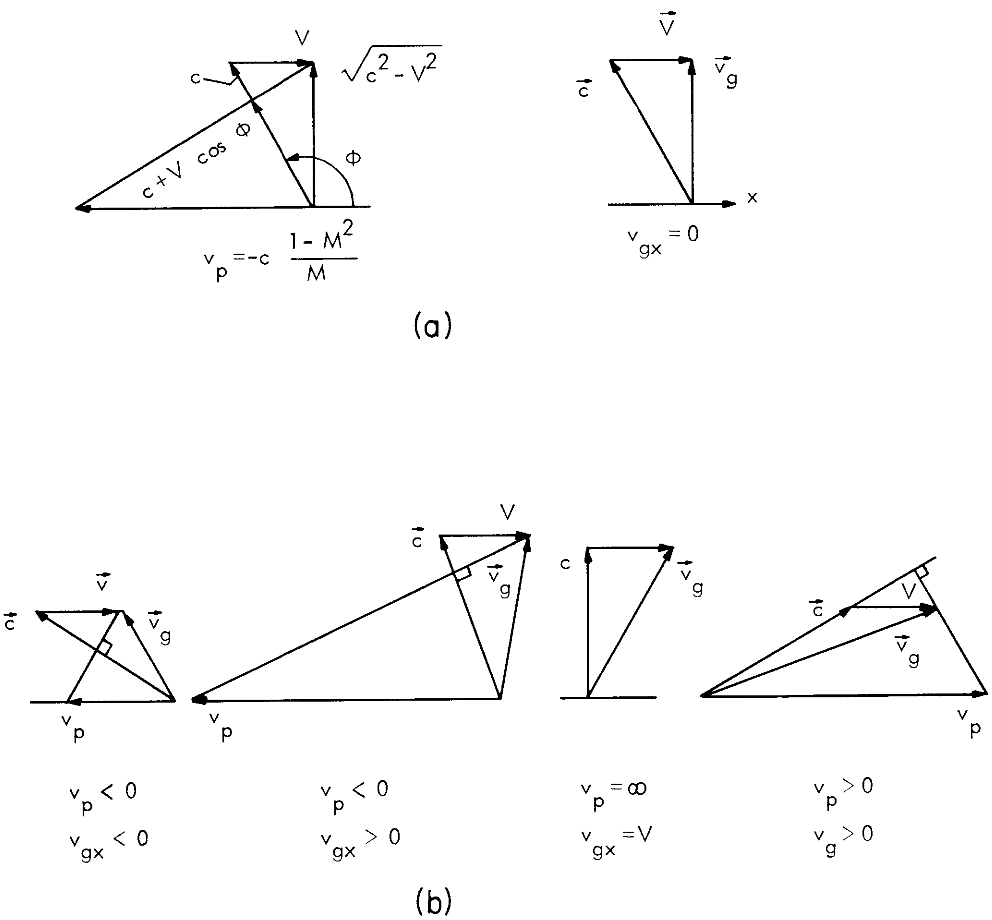

Fig. X-3. (a) Cutoff conditions that occur at frequency $\omega_c = ck_y \sqrt{1 - M^2}$. Group velocity is zero, $v_{gx} = d\omega/dk_x = 0$. Phase velocity is negative.
(b) Illustrating various conditions that can occur with regard to relative signs of group and phase velocities.

As the frequency is increased above the value ω_c, the plus and minus signs in Eq. 4 produce two different waves for each value of ω. Considering first the plus sign, we see that as the frequency increases, the phase velocity increases from its negative value at cutoff to approach the value c + V as ω increases. At the frequency given by $\omega/c = k_y$ we get $k_x = 0$ and an infinite phase velocity. This corresponds to propagation of the elementary plane wave perpendicular to the duct axis. The group velocity then is V, as can be seen from both the geometrical interpretation in Fig. X-3b and the analytical expression in Eq. 6.

Actually the frequency dependence of v_p and v_{gx} is indicated schematically in Fig. X-4 for both the (+) and (−) waves.

<u>Power-flow considerations.</u> The fact that the group velocity can be positive

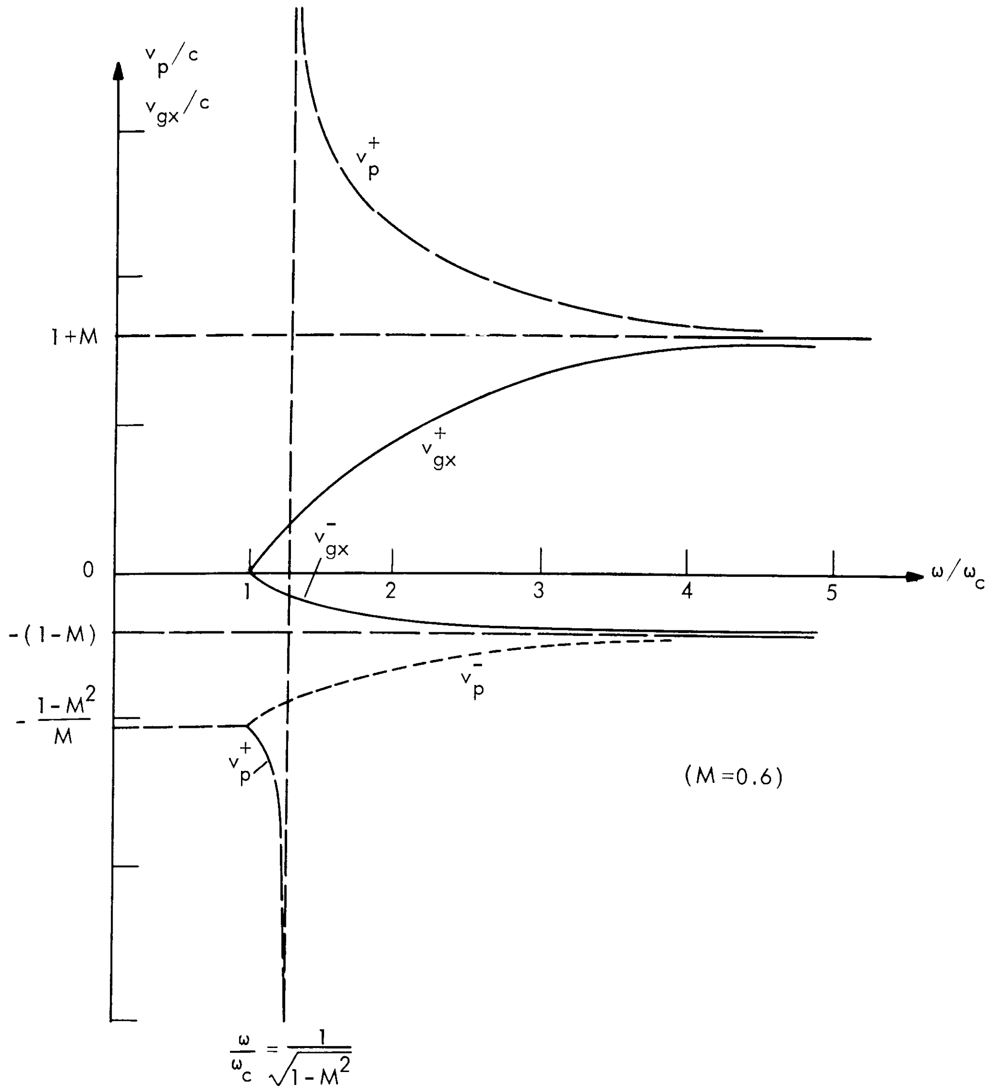

Fig. X-4. Frequency dependence of group and phase velocities. $\omega_c = ck_y \sqrt{1 - M^2}$.

even when the phase velocity is negative can have an important effect on the division of the power flow from a source between the upstream and downstream directions. First, it should be emphasized that the physically significant velocity is the group velocity. As a good approximation for the acoustic power flow per unit area we can use the expression

$$\vec{I} = W(\vec{c} + \vec{V}) = w\vec{v}_g, \tag{13}$$

where w is the energy density. Hence the group velocity determines the direction of the power flow.

This can be a significant factor to consider in many aircraft noise problems. Consider, for example, a point source in a duct which emits sound uniformly in

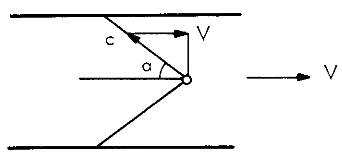

Fig. X-5.

Energy will be transmitted in the upstream direction only if the direction of the wave fronts lies within a cone with half the vertex angle given by $\cos \alpha = M$.

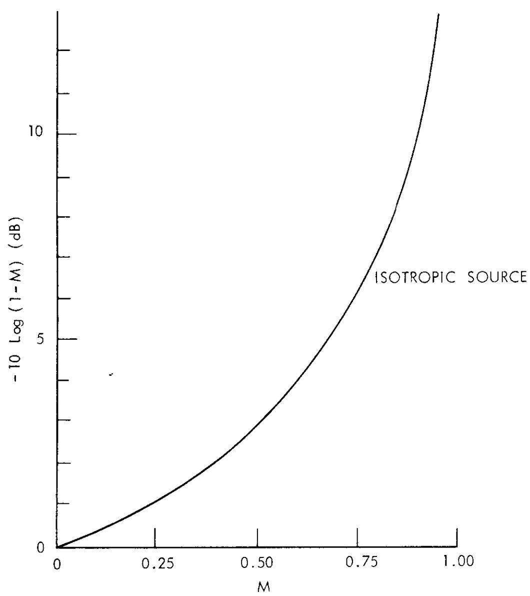

Fig. X-6.

Upstream radiation from an isotropically radiating source is reduced by a factor (1-M) as a result of the flow. The corresponding reduction (in dB) is shown as a function of M.

all directions, as indicated schematically in Fig. X-5. We have already seen that the group velocity is in the direction of the flow except for waves traveling within a cone in the upstream direction with a vertex angle given by

$$\cos \alpha = V/c = M. \tag{14}$$

The corresponding solid angle is $2\pi(1-\cos\alpha) = 2\pi(1-M)$. This effect of the flow is expected to reduce the emission of acoustic energy in the upstream direction by a factor (1-M). The corresponding reduction in decibels as a function of M is shown in Fig. X-6. It should be pointed out that this effect is a result of uniform flow and does not involve refraction caused by flow gradients.

6. Further Comments on Group Velocity and Energy Flow

As we have indicated, a higher mode in the duct is specified by k_y. Furthermore, if the frequency is specified, the corresponding propagation constant k_x for this mode is determined by Eq. 4. In any real situation, however, we are not concerned with a single frequency but rather a certain band of frequencies $\Delta\omega$. This spread in frequency produces a corresponding spread, Δk_x, in the propagation constant. (Also a spread in the Mach number can contribute to a spread in k_x.) For a given value of k_y, that is, for a particular mode, this spread in k_x can be thought of as a spread in the direction of propagation of the elementary plane waves that make up the mode in question. Since the direction of propagation for a given mode is given by $\tan \phi = k_y/k_x$, it follows that the spread in the angle ϕ is given by

$$\Delta\phi = -(\Delta k_x/k_x) \sin \phi \cos \phi. \tag{15}$$

Let us assume, then, that the sound source is such that in a certain frequency band the phase relationship between the individual frequency components can be maintained for a certain time. The corresponding radiation field resulting from the superposition of the frequency components in the band will then be a pulse or concentration of energy density moving along the duct with the group velocity. The behavior of a group of waves is frequently illustrated qualitatively by the addition of two plane waves with slightly different frequencies and corresponding wave numbers. We shall review this discussion and add a few remarks that are more closely related to the present problem.

If we start with the superposition of two mode components with slightly different frequencies ω and $\omega+\Delta\omega$ and corresponding values of k_x differing by Δk_x, the pressure field representing the sum is given by

$$p = \exp(ik_x x-i\omega t) + \exp(ik_x x-i\omega t+i\Delta k_x x-i\Delta\omega t)$$

$$\approx 2 \cos \frac{1}{2} (\Delta k_x x-\Delta\omega t) \exp i(k_x x-\omega t).$$

We have assumed that the waves have equal amplitudes, in both magnitude and phase. In the last exponential the quantities Δk_x and $\Delta\omega$ have been neglected compared with k_x and ω. It follows that the sum is a wave with a slowly varying amplitude. The peak amplitude, corresponding to $\Delta k_x x - \Delta\omega t = 0$, travels forward with a velocity given by $\Delta\omega/\Delta k_x$, which in the limit becomes $d\omega/dk_x$, the group velocity. The surfaces of constant phase, given by $k_x x - \omega t$ = constant, travel forward with the phase velocity ω/k_x. The pressure field in this particular rather artificial example has an infinite extent, although the amplitude varies.

This well-known result can be interpreted also in the following way. First, consider a single wave $\exp(ik_x x-i\omega t)$. The spatial dependence of this wave at a given time is $\cos (kx-\omega t_1)$. We can represent this spatial dependence by a vector as shown in Fig. X-7 in a manner completely similar to the conventional representation of the time dependence of a harmonic function, with the angle ωt replaced by kx. In other words, a displacement along the x axis equal to a wavelength corresponds to one complete rotation of the vector. The spatial dependence of the sum of two waves with

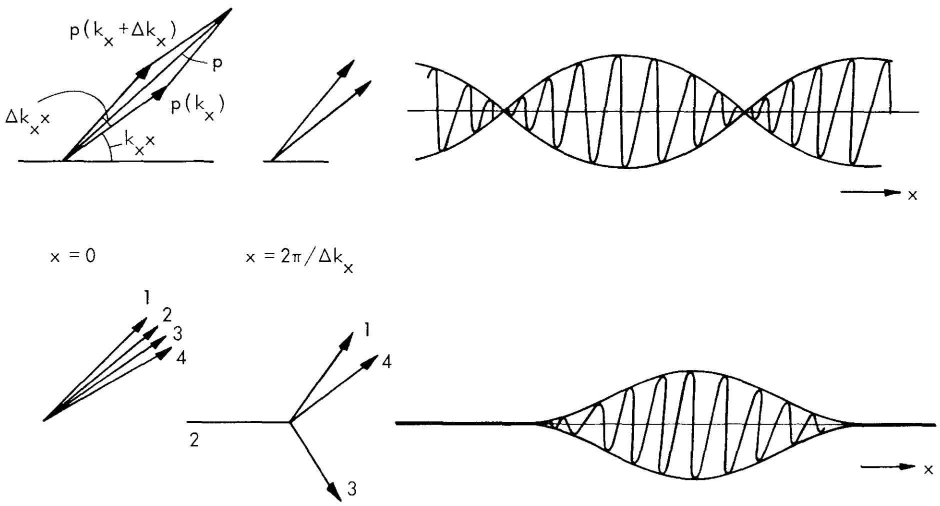

Fig. X-7. Illustrating superposition of waves with different propagation constants leading to wave groups (beats), using two waves, and to a wave pulse of finite extension resulting from a distribution of waves.

different wave numbers is represented by the sum of two vectors rotating with different speeds (see Fig. X-7). At a position where the two vectors coincide we have a maximum amplitude. As we proceed along the x axis from this point the vectors rotate but, since the wave numbers are different (difference Δk_x), they will separate and the resulting amplitude decreases. It will be zero when the vectors are opposite, but a further separation, corresponding to displacement

$$L = 2\pi/\Delta k_x$$

from the original position, brings the vectors to coincidence again, corresponding to a new maximum. This is nothing but the well-known distance between "beats."

Using the presentation shown in Fig. X-7, we can visualize what will happen when we have a continuum of wave vectors in the interval Δk, instead of having only two interfering waves. Such a group of waves will interfere constructively only over a distance of the order of $2\pi/\Delta k_x$, and this interference will not be repeated periodically as beats found in the case of two interfering waves. To see this, we start from the position where all the wave vectors have the same orientation (see Fig. X-7) and hence add up to a maximum. As we proceed away from this position, the wave vectors spread apart and their (vector) sum decreases, and this corresponds to a decrease in the wave amplitude. At a distance $2\pi/\Delta k$ the wave vectors are spread more or less uniformly between 0 and 2π, and the vector sum is close to zero. A further increase in distance will not bring the vectors together, and it follows that the constructive interference is limited to a region of length $2\pi/\Delta k_x$ centered about the maximum. Just as in the case of two interfering waves this region of constructive interference moves with the group velocity. The phase velocity has little significance in this connection.

It may be of interest in this context to interpret the interference within the wave group in still another way. A spread in Δk_x corresponds to a spread in the angle ϕ which relates to the direction of propagation of the plane waves that make up the higher order mode. In Fig. X-8 the wave fronts lying within the angular interval $\Delta\phi$ are indicated.

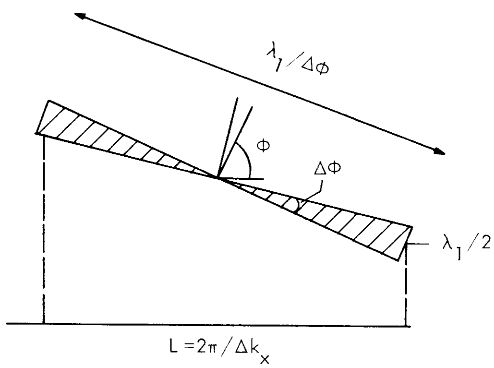

Fig. X-8.
Superposition of waves with different values of k_x can be interpreted as a superposition of plane waves traveling in different directions.

The constructive interference between these waves is confined to a region such that the distance between fronts is less than half a wavelength. Inside this region all wave components contribute with the same sign, if they are in phase at the center.

This interpretation is consistent with the previous discussion which indicated that the length of the wave region of constructive interference along the x axis is $2\pi/\Delta k_x$. From Fig. X-8 it follows that the projection on the x axis of the interference region is $(\lambda/\Delta\phi) \sin\phi$. But, according to Eq. 15, we have $|\Delta\phi| = (\Delta k_x/k_x) \sin\phi \cos\phi$. With $2\pi/\lambda = k_x/\cos\phi$ we find, as before, that length L is $2\pi/\Delta k_x$.

U. Ingard

B. BRAGG DIFFRACTION IN LANTHANUM FLINT GLASS

1. Introduction

The purpose of this project is to determine the acoustic properties of a sample of lanthanum flint glass relevant to its possible use in acousto-optic applications. This particular glass is of interest because of its high index of refraction. The acousto-optic figure of merit of a material[1] is proportional to n^6. Since glass is acoustically (as well as optically) isotropic, it offers advantages with respect to cost and design simplicity over a crystalline medium (which must be oriented to stringent specifications in order to ensure pure mode propagation).

Bragg diffraction of laser light can be used to determine the velocity and attenuation of ultrasonic waves in transparent samples. The sound waves modulate the refractive index, thereby creating an optical phase grating of spacing equal to the sonic wavelength. In Bragg diffraction, the light beam strikes the acoustic wave front at an angle such that it is scattered coherently from all points along the wave front. The Bragg angle in the sample is given by

$$\sin \theta = \lambda_{vac}/(2n\Lambda),$$

where λ_{vac} is the laser wavelength in vacuum, Λ is the acoustic wavelength, and n is the refractive index of the sample. Therefore, the velocity is given by

$$v = f\lambda_{vac}/(2n \sin \theta) \approx f\lambda_{air}/(2 \sin \Omega/2),$$

where $\Omega/2$ is the external Bragg angle (see Fig. X-9), and $\lambda_{air} = 6328.2$ Å.[2] Therefore, the sonic velocity is found directly by measuring the acoustic frequency and the Bragg angle.

The attenuation is measured by scanning the sample with the laser beam and directly measuring the spatial decay in the intensity of the scattered light.[1,3] The decrease in acoustic intensity at a distance x from the source of the sound wave is given by $I(x)/I(0) = \exp(-2\alpha x)$. Measurements were taken at several frequencies over the range 190-680 MHz.

2. Experimental Procedure

The sample is a rectangular block, $5 \times 2.5 \times 1$ cm, of Bausch & Lomb 867310 lanthanum flint glass of density 5.30 g/cm^3 and index of refraction 1.85036,[4] polished optically flat. An aluminum film was evaporated onto one end to serve as a ground electrode for the X-cut quartz transducer of approximate fundamental frequency 10.110 MHz, which is bonded to the sample with Dow resin 276-V2.

Figure X-9 shows the apparatus used in this experiment.[5,6] The sample is mounted on a calibrated divided-circle turntable. so that the Bragg angle can be read directly. The sample is placed in thermal contact with a temperature-controlled thermoelectric module. All measurements are made at 25°C, room temperature.

The light source is a 6328 Å He-Ne laser. The acoustic velocity is measured by setting the pulse generator to a harmonic frequency, finding the corresponding

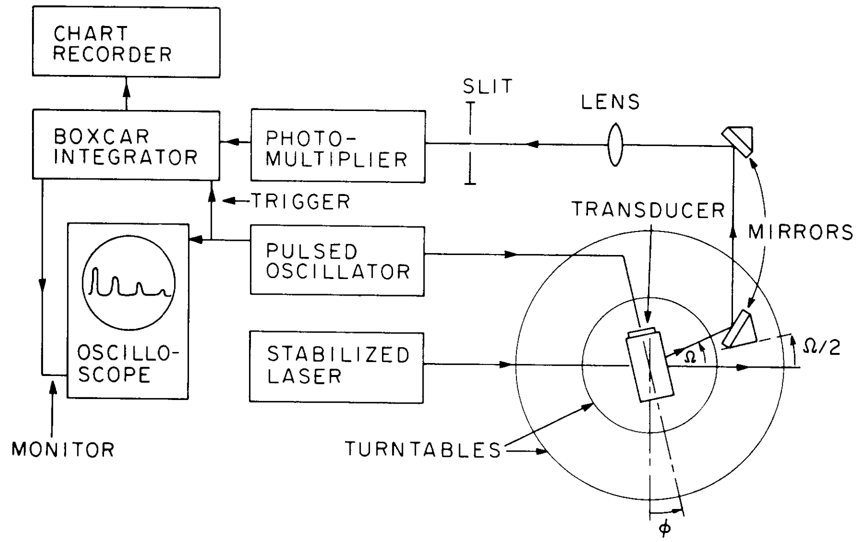

Fig. X-9. Experimental apparatus.

Bragg angle, and adjusting both to maximize the scattered intensity. Both the positive and negative Bragg angles are found. The average value is used in calculation, to remove errors caused by slight nonparallelism of the acoustic beam and the sides of the sample, and misalignment. The ultrasonic frequency is measured accurately by zero-beating the output of the pulsed oscillator with a transfer oscillator which, in turn, is measured by a crystal-stabilized frequency meter. A triple-stub tuner matches the transducer to the 50-Ω output impedance of the pulse generator.

In the attenuation measurements, the light beam is scanned along the length of the sample by using a micrometer drive to increment accurately the sample position with respect to the laser beam.[1,3] The amplified output of the photomultiplier is measured by a boxcar integrator and displayed on a chart recorder. The Bragg angle is adjusted for each reading to remove any misalignment caused by turning the micrometer.

3. Results

Data were taken at 20 transducer harmonics in the range 190-920 MHz. The values for the longitudinal velocity as a function of frequency and the resulting histogram are plotted in Fig. X-10. The longitudinal velocity is $(5.477 \pm 0.007) \times 10^5$ cm/s. The $\pm 1\sigma$ tolerance corresponds to a measurement accuracy of 0.14%.

The attenuation, as plotted in Fig. X-11, is given by A (dB/cm) $\sim f^{1.14 \pm 0.03}$, which is valid over the frequency range 190-680 MHz. This particular value is puzzling, since attenuation attributable to collisions of thermal phonons and structural relaxation should give an f^2 dependence. Data were taken up to the 91st harmonic, but at these points the attenuation was so high that meaningful data could be taken for a distance of 1 cm

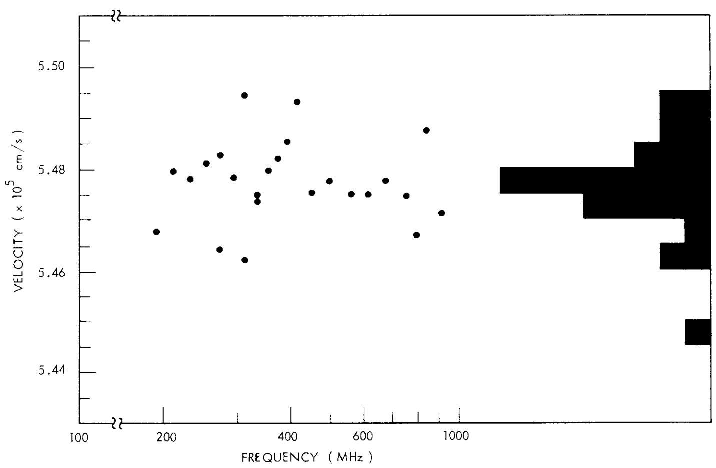

Fig. X-10. Distribution of measured velocity values as a function of frequency.

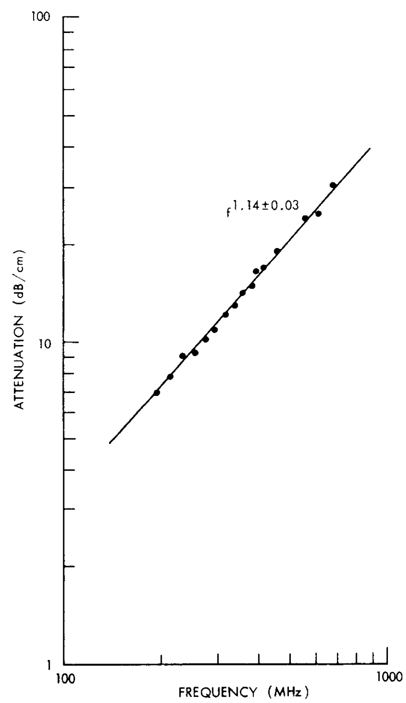

Fig. X-11. Ultrasonic attenuation as a function of frequency.

at most from the transducer, as opposed to a distance of 2.5 cm for the lower harmonics. Moreover, the points very close to the transducer are lost because the Bragg angle becomes so large at high frequencies that part of the sample holder blocks the diffracted beam. Another problem is that the feed-through from the pulsed oscillator is comparable to the height of the diffracted peak and tends to obscure it if the pulse is less than 2 mm from the transducer. This seriously cuts down the number of data points. More points might be found by using the boxcar integrator with a long time constant to follow a pulse into the noise, or by subdividing the distance.

4. Discussion

The important factors in accurately determining the sonic velocity are precise measurements of the Bragg angle and the acoustic frequency. Zero-beating the frequency allows it to be determined with an accuracy of 0.02% for a typical pulsewidth of 2 μs. The calibration of the turntable is accurate to ± 5 seconds of arc. The measured Bragg angles are in the range 35-190 min. Therefore the accuracy varies from 0.23% to 0.045% as the angle increases. The $\pm 1\sigma$ accuracy of the measurements was found to be 0.14%.

The largest source of error in the attenuation measurements arises in measuring the peaks. This is difficult as the signal-to-noise ratio becomes small and some noise is transmitted through the boxcar integrator. Another problem is improper maximization, which makes it necessary to reject some of the lower points. Nevertheless, the errors involved are small perturbations compared with the consistency of the results over a long range of measurement.

Lanthanum flint glass can probably be used in acousto-optic applications at freqencies as high as 300 MHz, at which the attenuation is 13.5 dB/cm. Further work will be done to extend the range of the attenuation measurements and measure the velocity of transverse waves. The values of the two velocities and of the density define the elastic constants of the material. When the photoelastic constant is measured, all factors in the figure of merit will be known.

J. F. Whitney, C. Krischer

References

1. M. G. Cohen and E. I. Gordon, Bell Syst. Tech. J. 44, 693-721 (1965).
2. K. D. Mielenz, H. D. Cook, C. E. Gillilland, and R. B. Stephens, Science 146, 1672 (1964).
3. C. D. W. Wilkinson and D. E. Caddes, J. Acoust. Soc. Am. 40, 498-499 (1966).
4. Bausch & Lomb Inc., Rochester, New York, Optical Glass Catalogue, n. d.
5. C. Krischer, Appl. Phys. Letters 13, 310-311 (1968).
6. C. Krischer, J. Acoust. Soc. Am. 48, 1086-1092 (1970).